

## Focused Magnetic Stem Cell Targeting to the Retina Using Superparamagnetic Iron Oxide Nanoparticles

Anat Yanai,\* Urs O. Häfeli,† Andrew L. Metcalfe,\* Peter Soema,†  
Lois Addo,\* Cheryl Y. Gregory-Evans,\* Kelvin Po,\* Xianghong Shan,\*  
Orson L. Moritz,\* and Kevin Gregory-Evans\*

\*Department of Ophthalmology & Visual Science, Faculty of Medicine, University of British Columbia, Vancouver, Canada

†Faculty of Pharmaceutical Sciences, University of British Columbia, Vancouver, Canada

Developing new ways of delivering cells to diseased tissue will be a key factor in translating cell therapeutics research into clinical use. Magnetically targeting cells enables delivery of significant numbers of cells to key areas of specific organs. To demonstrate feasibility in neurological tissue, we targeted cells magnetically to the upper hemisphere of the rodent retina. Rat mesenchymal stem cells (MSCs) were magnetized using superparamagnetic iron oxide nanoparticles (SPIONs). In vitro studies suggested that magnetization with fluidMAG-D was well tolerated, that cells remained viable, and they retained their differentiation capabilities. FluidMAG-D-labeled MSCs were injected intravitreally or via the tail vein of the S334ter-4 transgenic rat model of retinal degeneration with or without placing a gold-plated neodymium disc magnet within the orbit, but outside the eye. Retinal flatmount and cryosection imaging demonstrated that after intravitreal injection cells localized to the inner retina in a tightly confined area corresponding to the position of the orbital magnet. After intravenous injection, similar retinal localization was achieved and remarkably was associated with a tenfold increase in magnetic MSC delivery to the retina. Cryosections demonstrated that cells had migrated into both the inner and outer retina. Magnetic MSC treatment with orbital magnet also resulted in significantly higher retinal concentrations of anti-inflammatory molecules interleukin-10 and hepatocyte growth factor. This suggested that intravenous MSC therapy also resulted in significant therapeutic benefit in the dystrophic retina. With minimal risk of collateral damage, these results suggest that magnetic cell delivery is the best approach for controlled delivery of cells to the outer retina—the focus for disease in age-related macular degeneration and retinitis pigmentosa.

Key words: Magnetic targeting; Retina; Superparamagnetic iron oxide nanoparticles (SPIONs)

### INTRODUCTION

Retinal degenerations such as age-related macular degeneration, diabetic maculopathy, and retinitis pigmentosa account for the commonest causes of blindness in the developed world (10). Cell-based therapies, with their tissue regeneration potential (20,24) and paracrine effects (either innate or through genetic modification) (18,19,23,46), have many advantages over other treatment modalities. As such cell therapies move towards clinical trials, an increasingly important issue is how best to target cells to diseased tissue. Critical considerations include the potential for collateral damage within the tissue, systemic side effects, local tissue barriers (such as the blood–brain barrier and blood–retina barrier), ease of delivery method, repeatability, and whether

specific loci within the tissue need to be targeted. This latter point is particularly important in diseases of the central nervous system. In the human retina, for example, regional differences in tissue function can make therapy targeted randomly at the tissue or with the intention to uniformly cover the entire tissue suboptimal. For example, in age-related macular degeneration, cell therapy needs to be directed specifically at the macular region of the retina since cells delivered into the peripheral retina will have no functional benefit or might even disrupt normal tissue function. Direct injection of cells into the macula, while feasible, is associated with significant risk of complications and makes repeated treatments to a large extent impractical (2,39).

Remote cell delivery via the systemic circulation would be advantageous; however, this technique has had

---

Received January 12, 2011; final acceptance July 14, 2011. Online prepub date: March 8, 2012.

Address correspondence to Kevin Gregory-Evans, M.D., Ph.D., FRCS, FRCOphth., Centre for Macular Research, Department Ophthalmology and Visual Sciences, University of British Columbia, 2550 Willow Street, Vancouver, BC, Canada V5Z 3N9. Tel: +1-604-671-0419; Fax: +1-604-875-4663; E-mail: [kge30@eyecarecentre.org](mailto:kge30@eyecarecentre.org)

limited success (25,28). In the eye, although intravenous mesenchymal stem cells (MSCs) have been shown to reach the retina, this has only been in very low numbers and in a random distribution (44). Recently, a number of studies have looked at magnetic targeting of cells. In vivo studies have shown that magnetic labeling, particularly with superparamagnetic iron oxide nanoparticles (SPIONs), is relatively easy and safe (22,41,42). However, limited work has been done on using magnetic fields to guide SPION-labeled cells to specific targets (45). Mostly these have concentrated on delivering cells to the systemic vasculature (7,21,32–34). One study has shown that SPION-treated MSCs accumulate in the normal liver of rats after intravenous injection when an external magnet is placed over the abdomen (1). Again, though, only in low numbers and only to the most superficial liver tissue. One study has shown that magnetized cells injected into the cerebrospinal fluid (29) can be moved within the spinal column to advantage. As yet, however, no study has assessed the ability of magnetized cells to home into specific CNS targets after injection into the systemic circulation.

Overall, it has yet to be established that magnetic delivery of cells via the systemic circulation can deliver enough cells to target tissues. If this could be achieved, other potential advantages such as precise localization, repeatability, and minimal local collateral damage would make further clinical studies worthwhile. With focal retinal diseases such as age-related macular degeneration in mind, we therefore undertook an in vivo study to establish whether SPIONs could be used to guide intravenously injected MSCs to a specific retinal locus.

## MATERIALS AND METHODS

### *Cell Culture, Labeling, and Characterization*

MSCs were isolated from bone marrow. Briefly, bone marrow cells from both femurs of a single rat were flushed with 2–5 ml of knockout DMEM, centrifuged for 5 min at  $1,200 \times g$ , resuspended in growth media (DMEM supplemented with 10% fetal bovine serum, 2 mM L-glutamine, and 100 U penicillin/streptomycin), and maintained at 37°C in a humidified 5% CO<sub>2</sub> incubator. All reagents were supplied by Invitrogen.

FluidMAG-nanoparticles (Chemicell, Berlin, Germany) are ferrofluid, 200-nm-diameter particles composed of a magnetite core covered by hydrophilic polymers protecting against aggregation. We studied fluidMAG-DXS (coated with dextran sulfate) and fluidMAG-D (coated with starch) particles. After passaging, cell suspensions were incubated with aqueous suspensions of each particle for 2 h in a T75 flask. An oblong magnet was then attached to the underside of the flask. After overnight incubation cells were stained with crystal violet to determine which cells had preferentially localized over the

magnet. The viability of unlabeled MSCs and those incubated with SPIONs was analyzed by 3-[4,5-dimethylthiazol-2-yl]-2,5-diphenyltetrazolium bromide (MTT) assay (14). Briefly, MSCs in a 96-well plate (10,000 cells/well) were incubated in 100 µl growth media for 24 h. Varying concentrations of SPIONs were added to the wells and after 24 h MTT (Sigma) was added for 1 h. The media was removed and cells were incubated for 1 h in the presence of dimethyl sulfoxide (DMSO; Sigma). The absorbance at 560 nm was determined on a U-Quant Plate Reader (Bio-Tek Instruments). The adipogenic differentiation ability of unlabeled MSCs and SPION-labeled MSCs was assessed using the MesenCult® Adipogenic Stimulatory kit (Stemcell Technologies, Vancouver, Canada) following the manufacturer's instructions. The resulting adipogenic cells were visualized using Oil Red O staining (Sigma). Osteogenic differentiation was assessed using the MesenCult® Osteogenic Stimulatory kit (Stemcell Technologies). Resulting osteoblast cells were visualized using Von Kossa staining (Sigma).

To evaluate SPION uptake, MSCs were cultured on 3-µm polyester membranes (Corning) and processed for transmission electron microscopy. Briefly, the samples were infiltrated with Spurr's low viscosity resin and embedded in flat-bottomed Beem capsules. Thin sections were stained for 12 min with uranyl acetate and 6 min with Reynold's lead citrate before imaging using an FEI Tecnai G2 20 TWIN. To determine the iron load carried by SPION-treated MSCs, 50-ml aliquots containing  $1.0 \times 10^6$  treated or untreated MSCs were suspended in distilled water and underwent inductively coupled plasma atomic emission spectroscopy (Exova, Surrey, Canada). These experiments were done in triplicate.

In preparation for in vivo use, MSC cultures (containing cells at passage 4–9) were incubated for 24 h with 10 µl SPION and 2.5 µl Q-Tracker® 655 (Invitrogen), a fluorescent marker for identifying labeled cells in tissue sections. Cells were then washed eight times with DPBS (Invitrogen) and then detached with 0.05% trypsin EDTA (Invitrogen). MSCs were stained with trypan blue stain 0.4% (Gibco), counted, and then  $1.0 \times 10^6$  cells were suspended in 1 ml DPBS for injection.

### *Animal Studies*

The S334ter-4 heterozygous transgenic rat line (obtained from Professor Matt LaVail, University of California at San Francisco, CA, USA) was used since it is a well-characterized model of retinal degeneration (5,8,11,13,40). Animals were maintained on a 12-h light/dark cycle and research carried out with adherence to the Association for Research in Vision and Ophthalmology Statement for the Use of Animals in Ophthalmic and Vision Research and local Institutional Animal Care Committee Regulations.

Animals underwent general anesthesia using 2–3% isoflurane. A 3-mm diameter  $\times$  1.5-mm-thick gold-plated neodymium iron boron (NdFeB) disc magnet with a maximum energy product of 43.2 MGOe (D0301G, Gaussboys Super Magnets, Portland, OR, USA) was placed within the orbit, but outside the eye, in selected animals. A 2-mm limbal incision was made in the superior fornix and the magnet was pushed back into the orbital apex with a nonmagnetic blunt probe. Using a Hamilton syringe, 4  $\mu$ l of the SPION-treated MSC suspension ( $2 \times 10^5$  cells) was injected into the vitreous cavity of one eye, through an entry site 1–2 mm behind the limbus of the eye (6). Other animals underwent intravenous tail vein injection of 1 ml DPBS vehicle alone or containing approximately  $1.0 \times 10^6$  SPION-treated MSCs.

### Histology

Rat eyes were enucleated, anterior segments were removed, and posterior eyecups fixed in 4% paraformaldehyde for 1 h at 4°C. Neurosensory retina flatmounts were obtained by blunt dissection of retina from these eyecups, flattening the tissue onto Superfrost Plus microscope slides (Fisher), and mounting under a coverslip with Fluoromount-G (Southern Biotech). Cryosections of tissue were obtained either by reprocessing flatmounts or, when studying the outer retina, by processing fresh eye cup tissue. Briefly, posterior eyecups were fixed with 50% Karnovsky's fixative (2.5% glutaraldehyde, 2% paraformaldehyde, 0.03 M sodium cacodylate, pH 7.4) for 1 h and then transferred to PBS containing 25% sucrose and incubated for ~8 h. Flatmount tissue or eyecups were embedded in O.C.T medium (Tissue-Tek; Torrance, CA) and 14–16- $\mu$ m sections were obtained using a cryostat (Microm HM 525; Waldorf, Germany). Before imaging, O.C.T was removed by washing with PBS for 10–15 min and nuclei were labeled with Hoechst (Sigma; 10  $\mu$ g/ml in 0.1% Triton X-100/PBS) for 5 min, followed by three washes in PBS and mounting in Fluoromount-G. To assess whether labeled MSCs also appeared in other organs, cryosections were obtained from tissue samples from bone marrow, lung, liver, and spleen. Confocal images of flatmounts and cryosections were acquired using a Zeiss LSM 510 META confocal laser scanning system attached to a Zeiss Axiovert 200M inverted microscope. Multiple images from individual tissue samples were combined to form image montages.

### Enzyme-Linked Immunosorbent Assay (ELISA)

Isolated neurosensory retinas from rat eyes were homogenized with a 25-gauge needle using 200  $\mu$ l cold PBS. Homogenates were then centrifuged for 10 min at  $13,000 \times g$  and growth factor concentration was determined in the cleared supernatant using a sandwich

ELISA. ELISA kits for glial-derived neurotrophic factor (GDNF; Emax® ImmunoAssay System, Promega, Madison, WI), ciliary neurotrophic factor (CNTF; RayBiotech, Norcross, GA), interleukin-10 (IL-10; Abnova, Taipei City, Taiwan), and hepatocyte growth factor (HGF; B Bridge, Cupertino, CA) were each used according to the manufacturer's instructions. Visualization of the chromogenic substrates was measured at 450–490 nm using a U-Quant Plate Reader (Bio-Tek Instruments). All samples were analyzed in duplicate and results were calculated as pg/ml.

### Image and Statistical Analysis

We elected to determine whether magnetic MSCs could be selectively delivered to the upper hemisphere of the retina (corresponding to the positioning of the orbital magnet). Flatmount retinal images were used to study magnetic MSC retinal coverage. To standardize the retinal area assessed, flatmount images were edited in Photoshop (Adobe) to include only the upper hemisphere of the central 7-mm diameter of retinal tissue, centered on the optic nerve head. To isolate Q-Tracker 655 signal (derived from magnetic MSCs), the red channel of each image was isolated. Percentage of retinal area covered by Q-Tracker 655 signal was then calculated using ImageJ software. Data were collated as the median value with upper and lower quartiles. These quartiles were calculated by using the median value to divide the ordered data set into two halves. The median value was then included in both halves. The lower quartile (LQ) was calculated as the mean of the lower half of the data and the upper quartile (UQ) as the mean of the upper half of the data. A Mann-Whitney *U*-test was used to determine statistical significance. Total MSC counts in the retina were calculated by dividing these calculations of surface area of Q-Tracker signal in flatmounts by the average surface area of Q-Tracker signal from single MSCs in retinal sections.

Data from ELISA experiments was also collected and compared as median with LQ and UQ and a Mann-Whitney *U*-test was used to determine statistical significance (set as  $p \leq 0.05$ ).

## RESULTS

### *Magnetizing MSCs and Effects on Cell Viability*

MSCs in cell suspension avidly internalized SPIONS as demonstrated by cells moving towards a magnetic source, within 12 h of treatment. To determine which SPION was most efficacious in magnetizing MSCs, a magnet was placed under culture flasks, before treated cells had become adherent, to semiquantitatively assess the numbers of cells that preferentially localized near to the underlying magnet. After 18 h, these treated MSC cultures were stained with crystal violet (Fig. 1). The

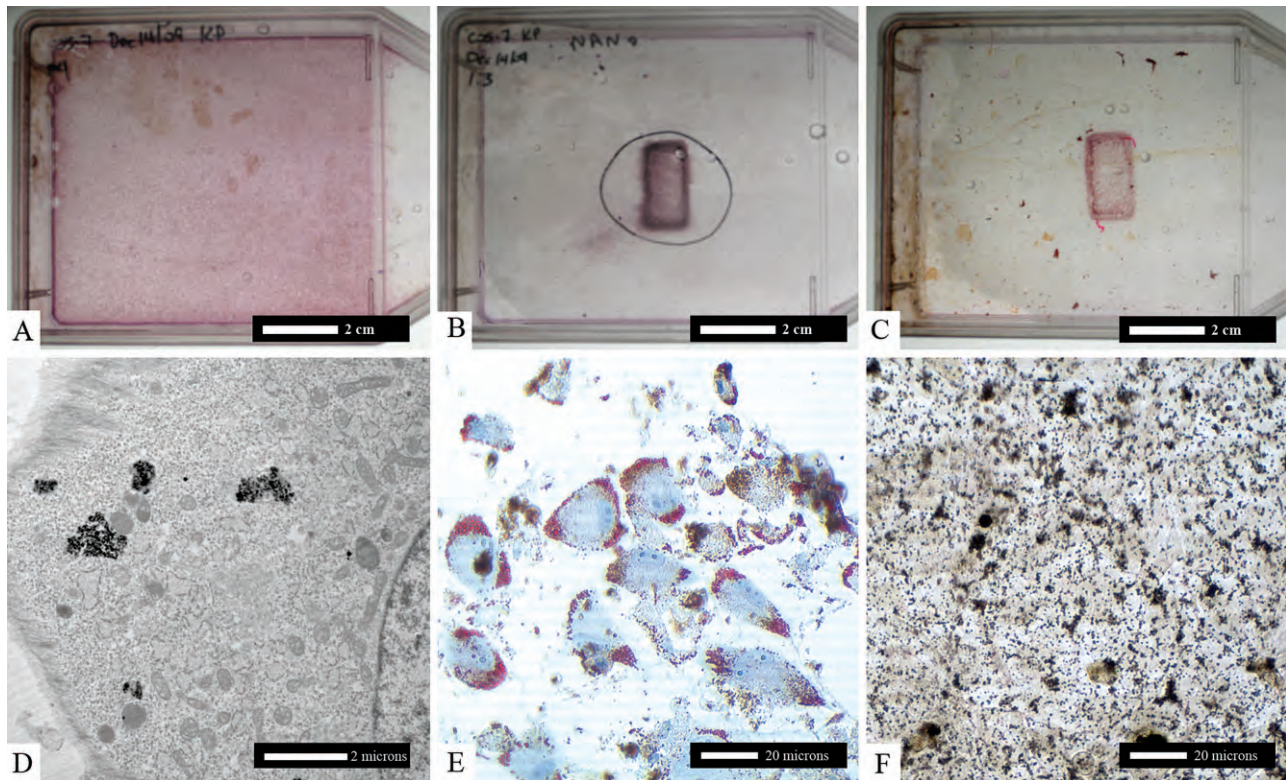


**Figure 1.** Mesenchymal stem cell (MSC) culture with superparamagnetic iron oxide nanoparticles (SPIONS). (A) MSC culture, no magnet. (B) MSC containing fluidMAG-D (coated with starch) SPIONS plus magnet. (C) MSC containing fluidMAG-DXS (coated with dextran-sulfate) SPIONS plus magnet. (D) Transmission electron micrograph showing fluidMAG-D particles accumulation within aggregates in MSCs. (E) FluidMAG-D-treated MSCs differentiated into adipocytes (Oil Red O staining). (F) FluidMAG-D-treated MSCs differentiated into chondrocytes (brown deposits).

most intense staining was seen in flasks treated with fluidMAG-D (Fig. 1B), suggesting that these treated cells were the most responsive to magnetic attraction. Emission spectroscopy suggested that on average, each fluidMAG-D-treated MSC contained approximately 7 pg of iron oxide, whereas MSCs incubated with fluidMAG-DXS resulted in an iron oxide content of 10 pg/cell (data not shown). FluidMAG-D nanoparticle uptake by rat MSCs was visualized by transmission electron microscopy, which showed particles localizing within aggregates throughout the cytoplasm (Fig. 1D).

MTT assays were undertaken to assess MSC viability after SPION treatment (Fig. 2). This suggested that fluidMAG-D treatment was best tolerated by cells. After 24 h, over 95% of MSCs were still viable when using fluidMAG-D at concentrations of 0.05, 0.25, or 0.5 mg/ml in culture media. When fluidMAG-DXS particles were used, significantly poorer cell survival was documented at 24 h (e.g., at a concentration of 0.05 mg/ml, only 68% cell survival was seen in comparison with 100% survival seen with fluidMAG-D) (Fig. 2). We

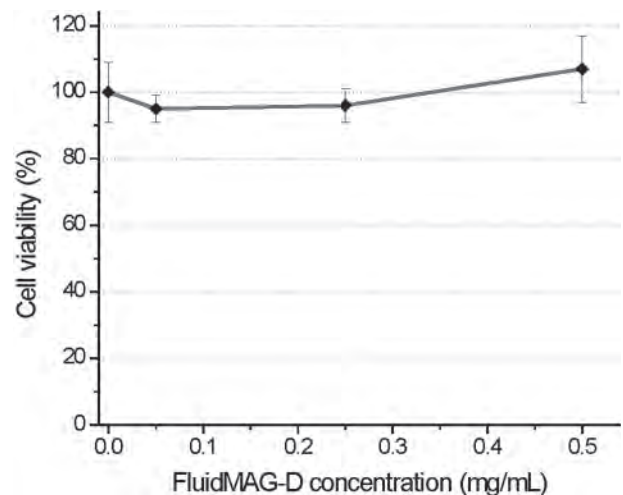


**Figure 2.** MTT assay. Mesenchymal stem cell viability 24 h after addition of fluidMAG-D to tissue culture supernatant. Each data point represents mean survival in eight separate measurements. Error bars correspond to SEM.

therefore elected to use fluidMAG-D in further experiments and at a concentration of 0.05 mg/ml fluidMAG-D to minimize carryover of unincorporated SPIONS in cell culture suspensions. Additionally, we undertook experiments to examine whether SPION treatment interfered with MSCs normal differentiation capacity. FluidMAG-D-treated MSCs were seen to retain their ability to differentiate into adipocytes (Fig. 1E) and osteocytes (Fig. 1F), suggesting that cells retained the characteristics of MSCs even after 4 weeks incubation with fluidMAG-D particles.

#### *Intravitreal MSC Delivery*

To investigate the distribution of fluidMAG-D (magnetized) MSCs labeled with Q-Tracker 655 *in vivo*, the retinal surface was examined by flatmount imaging 1 week after intravitreal injection into rat eyes. Intravitreal injection led to a random distribution of fluidMAG-D MSCs over the retinal surface (Fig. 3), with most cells preferentially adhering to the posterior lens surface (data not shown). In comparison, when an orbital magnet had been placed into the eye prior to intravitreal injection, a highly concentrated accumulation of cells in the upper retinal hemisphere was seen (Fig. 3B). In these eyes the cells appeared to aggregate in a circle corresponding to the perimeter of the orbitally placed magnet. This reflected the maximum gradient in magnetic field (the largest magnetostatic forces experienced by magnetic particles) found at the edges of a magnet, when it has been uniformly magnetized along its axis (17). Image processing and quantification in three eyes containing an orbital magnet confirmed that eyes treated with magnetized MSCs demonstrated a statistically significant accumulation of cells in the upper hemisphere of the retina with a median 20.0% coverage (LQ 19.5, UQ 20.45) compared with lower hemisphere retina median coverage 0.25% (LQ 0.05, UQ 1.5;  $p < 0.05$ ). Significant accumulation of cells was also demonstrated when comparing upper hemisphere images in eyes with a magnet (data above) and without an orbital magnet being present (0.6% coverage, LQ 0.25, UQ 0.55;  $p < 0.05$ ,  $n = 3$ ). This corresponded to an increase in MSC targeting to the upper retina from 9,600 to 355,500 cells if a magnet was positioned in the upper orbit. Retinal cryosections demonstrated that magnetic MSCs aggregated in clumps on the inner retinal surface (Fig. 4), with a few cells present in ganglion cell layer (arrows). No magnetic MSCs were however identified in deeper retinal layers.

#### *Intravenous MSC Delivery*

To determine whether systemic delivery of MSCs could also be targeted to the retina, rats were injected with a suspension of magnetized, Q-Tracker-labeled

MSCs into their tail vein. Retinal flatmount images again identified magnetic MSCs preferentially distributed in the upper retinal hemisphere, around an area corresponding to the orbitally placed magnet, but with less intensity than seen with the intravitreal injection (compare Fig. 3D and B, respectively). Similarly at 1 month after injection, cells were also present in the upper retinal hemisphere (Fig. 3F). Image processing of upper hemisphere retinal images of five eyes treated with magnetic MSCs and an orbital magnet suggested 2.48% coverage at 1 week (LQ 1.75, UQ 2.8) and 0.61% at 1 month (LQ 0.05, UQ 1.0). This was significantly more than seen in eyes treated with magnetic MSCs only at both 1 week (0.25%, LQ 0.11, UQ 0.28;  $p < 0.05$ ) and 1 month (0.07%, LQ 0.01, UQ 0.8;  $p < 0.05$ ). This corresponded to an increase in MSC targeting to the upper retina from 4,000 cells to 42,000 cells if a magnet was positioned in the upper orbit, a 10-fold increase in cell delivery at 1 week.

Retinal cryosections identified numerous Q-Tracker-labeled cells distributed within the retina. Of note, after 1 week, magnetic MSCs could be detected only in the inner retina if no magnet had been placed in the orbit (Fig. 4B–E). In comparison, magnetic MSCs could be identified in both the outer (Fig. 4F–H) as well as the inner retina if a magnet had been placed in the orbit. Similar findings were obtained in retinal tissue examined 1 month after treatment. It was also noted that magnetic MSCs appeared in vitreous strands (condensations of membranes normally seen within the semigelatinous vitreous humor that fills the cavity of the eyeball between the retina and lens). This was regardless of whether or not a magnet had been placed in the orbit (Fig. 5). MSCs also appeared to distribute around the body. After intravenous injection, magnetic MSCs could be identified in cryosections obtained from the liver, spleen, and bone marrow. Magnetic MSCs could also be detected in cryosections from lung tissue if no magnet had been placed in the orbit (data not shown).

These positive results with intravenous injection of magnetic MSCs led us to determine whether systemic treatment resulted in a biochemical effect in dystrophic retina. ELISA results suggested that, when compared to untreated retina, magnetic MSC treatment was associated with significantly increased retinal concentrations of IL-10, HGF, and CNTF at 1 week and 1 month ( $p < 0.05$ ,  $n = 3$ ) (Fig. 6). For neuroprotectant molecule GDNF, a statistically significant increase was seen at 1 month only compared to untreated retina ( $p < 0.05$ ,  $n = 3$ ). However, upon comparing eyes treated with magnetic MSCs either with or without an orbitally placed magnet, statistical significance was only achieved when measuring IL-10 and HGF concentrations ( $p < 0.05$ ). This suggested that MSC therapy resulted in enhanced

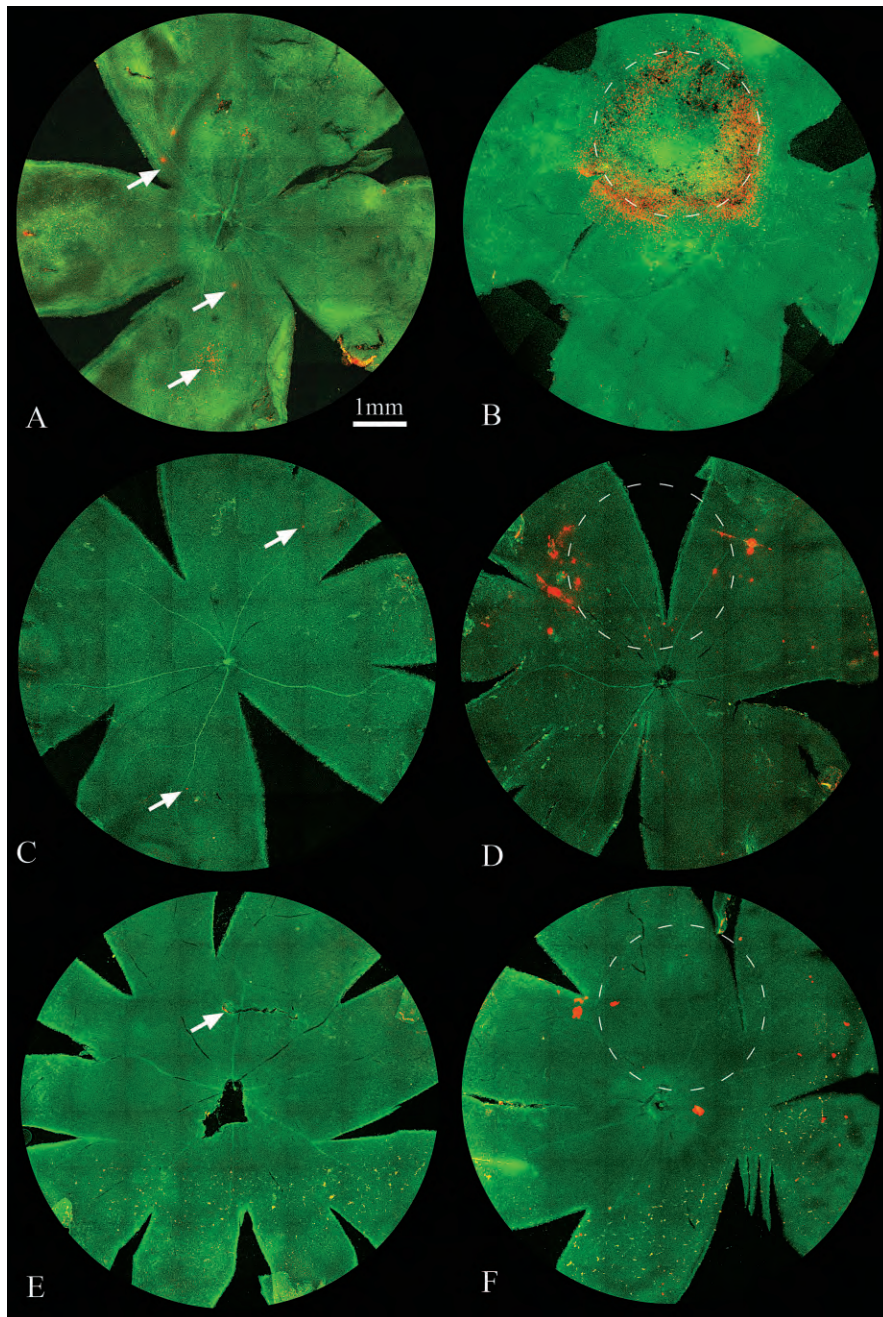


**Figure 3.** Flatmount images of S334ter-4 rat retina injected with magnetic MSCs. (A, C, E) No magnet. (B, D, F) With magnet. (A, B) One week after intravitreal injection. (C, D) One week after intravenous injection. (E, F) One month after intravenous injection. Arrows indicate small areas of magnetic MSCs in retina without a magnet. Dashed white circle shows the position of the magnet.

retinal concentrations of all four molecules, but magnetic targeting improved upon this only for IL-10 and HGF.

#### DISCUSSION

We have shown for the first time that large numbers of MSCs can be targeted to a preselected area of the

dystrophic retina without the need for invasive intraocular surgery. Specifically, we have seen that magnetized cells will preferentially accumulate within the upper hemisphere of the retina, demonstrating that an externally placed magnet can be used to direct MSCs tangentially, over the retinal surface. Importantly, it was also found that this technique can also control where cells

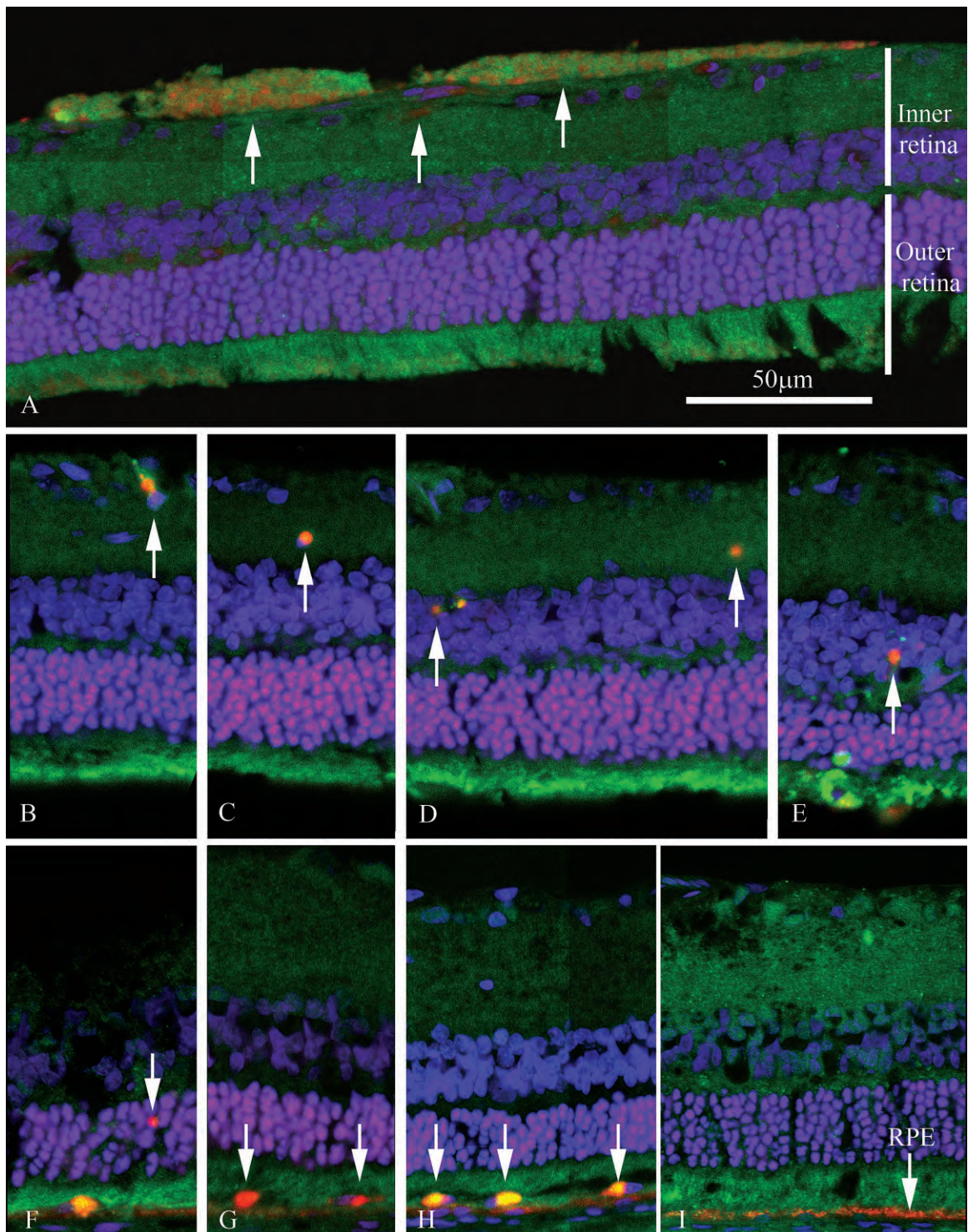


**Figure 4.** Retinal cryosections. (A) After intravitreal injection, MSCs accumulate (white arrows) on retinal surface (Q-Tracker labeled red). (B–E) MSCs in the inner retina 1 week after therapy, no magnet. (F–H) MSCs in the outer retina with magnet. (I) Control, intravenous vehicle only. RPE, red autofluorescence in the retinal pigment epithelium and Bruch's membrane.

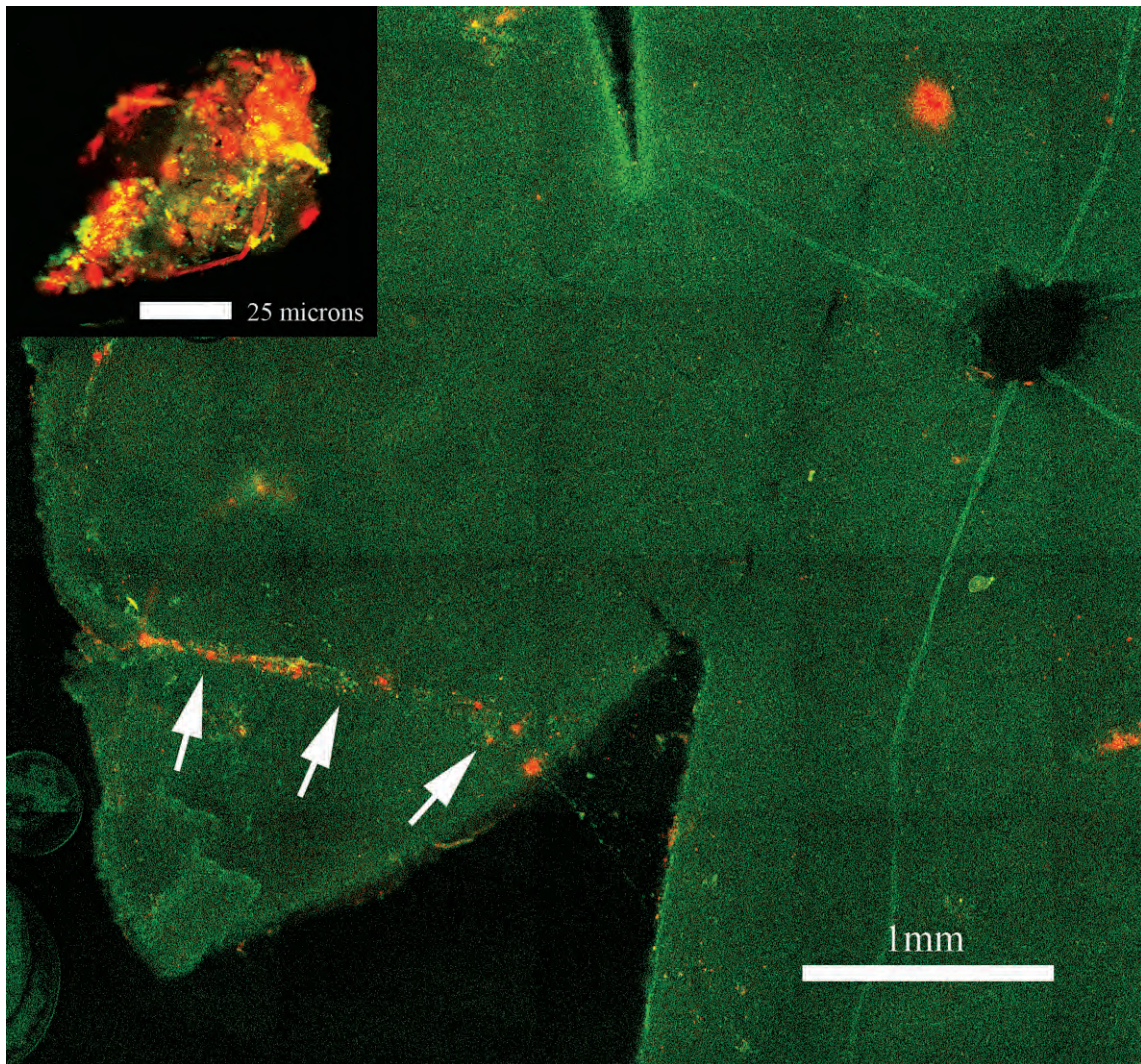


**Figure 5.** Flatmount retinal image showing Q-Tracker-labeled cells (red) adherent to vitreous strands (arrows). Inset: vitreous sample showing Q-Tracker signal suggesting magnetic cells accumulate in the vitreous as well as the retina with or without placing a magnet in the orbit.

were delivered cross-sectionally, within the retinal layers. This latter advantage is particularly advantageous since common retinal diseases (such as age-related macular degeneration and retinitis pigmentosa) particularly affect the outer retina. No other cell delivery method apart from subretinal injection, with its attendant risks and limited repeatability (39), has been shown to be able to efficiently target the outer retina (23) without the need to chemically disrupt tissue boundaries (31). Magnetic targeting of MSCs is also a significant improvement on previous studies using intravenously injected, unlabeled MSCs into the dystrophic retina (44). In that study, it was found by semiquantitative RT-PCR that there were increased levels of CNTF and BDNF [but not basic

fibroblast growth factor (bFGF)] in treated retina. It was noted, however, that cells distributed randomly to the peripheral rather than central retina; no quantitative assessment of MSC delivery to the retina was made; and immunohistochemistry showed that MSCs could only be detected in the inner retina (44).

One concern with our conclusions based on labeling cells with Q-Tracker 655 is that this cell marker may escape from labeled MSCs into surrounding cells. Previous studies using bone marrow MSCs in the eye, however, suggest that this is unlikely (6) and if present would result in only very low concentrations of Q-Tracker 655 in surrounding cells. Such minimal tissue staining would likely be below the detection ability of

our imaging equipment. Another concern is that labeled MSCs, localized within the retina, may undergo division and so affect cell counts. MSCs do proliferate after *in vivo* injection (27) and more specifically in the eye; there is evidence to suggest that lineage-negative bone marrow cells (which would include MSCs) injected into the vitreous cavity do undergo some division (43). This effect is likely to be small, however, since over time MSCs differentiate and lose their proliferative capacity (27,30).

MSCs are remarkable in stem cell biology. With significant retinal regeneration potential (3), more recently their paracrine effects on the retina have become increasingly recognized as useful therapeutic approaches (47). In particular, clinical roles for MSC therapy in retinal neuroprotection and immune suppression have been

proposed (18). Systemically delivered MSCs therefore have significant potential for delivering neuroprotective and anti-inflammatory molecules to the diseased retina, although our study may suggest that magnetic MSCs show most potential in enhancing anti-inflammatory effects in the retina (i.e., through increased retinal concentrations of IL-10 and HGF). It has been suggested that with MSC therapy, elevated concentrations of neuroprotective molecules such as CNTF derive from secondary Müller cell secretion rather than from MSCs *per se* (44). Despite enhanced MSC delivery as a result of magnetic targeting, that GDNF and CNTF concentrations were not elevated further may suggest a plateau response, with CNTF release determined by fixed tissue factors (e.g., number of Müller cells) rather than MSC concentration. Such a phenomenon might be relevant to

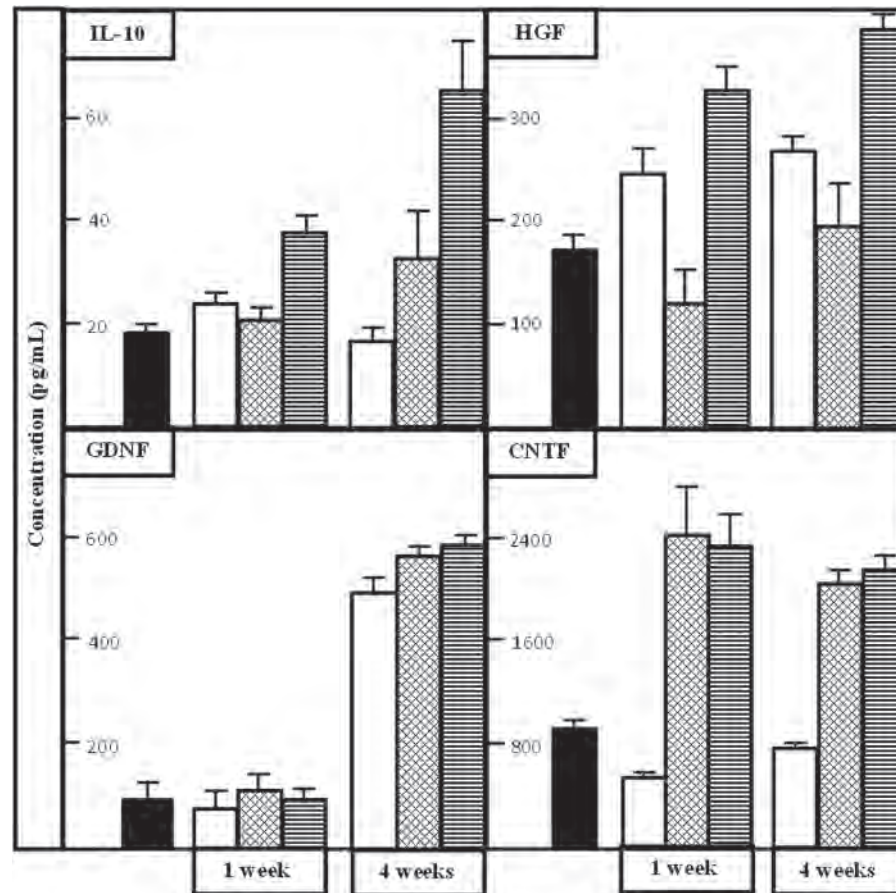


**Figure 6.** ELISA results from retinal tissue. Measurements taken at the P90 time point after either 1 week or 1 month of treatment to determine tissue concentrations of anti-inflammatory [interleukin-10 (IL-10), hepatocyte growth factor (HGF)] and neuroprotectant molecules [ciliary neurotrophic factor (CNTF), glial derived neurotrophic factor (GDNF)]. Black bar: untreated; white bar: animals treated with vehicle only; cross-hatched bar: treated with magnetic MSCs, no magnet placed in orbit; horizontal shading: treated with magnetic MSCs, plus magnet placed in orbit. Error bars represent upper quartile value. For each data point  $n = 3$ .

MSC therapy in other organs and may explain poorer neuroprotective effects in clinical studies than predicted from *in vitro* and preclinical work (30).

The relevance of MSC detection in other organs as well as the eye is of uncertain significance. Only random samples of extraocular tissues were selected for cryosection analysis so a quantitative assessment was not possible. That no magnetic MSCs were detected in lung tissue after placing an orbital magnet may therefore represent a sampling error. No study has yet reported significant adverse effects with systemic delivery of MSCs. In addition, since MSCs are differentiated cell lines, risks of neoplasia would seem minimal. Further studies, for example using radiolabeled magnetic MSCs, would more efficiently assess the systemic distribution of intravenously injected magnetic MSCs. Furthermore, the appearance of magnetized MSCs in the vitreous after systemic administration has not previously been reported. The consequences of this are also unknown, although cellular infiltrate into the vitreous could stimulate fibrosis and retinal traction (12). Further studies need to be undertaken to explore these phenomena.

Some evidence has suggested that SPION treatment and subsequent exposure to magnetic fields alters cell metabolism (9,16,26). More specifically, *in vitro* MSC studies using SPIONs have shown a range of effects (37,38). A recent study of human MSCs showed that Resovist treatment and exposure to magnetic fields reduced cell proliferation and increased the MSCs ability to differentiate into adipocytes (36). Additionally, in an animal model of multiple sclerosis, MSC therapy worsened rather than improved symptoms if the MSCs had been labeled with SPIONs (35). More recent work, however, has suggested that SPIONs do not affect MSC differentiation (4). In our work, fluidMAG-D treatment had no short-term effects on cell viability or differentiation ability. Longer term studies are required to explore this further.

Results presented here show that blood-borne magnetic MSC targeting to specific tissue loci is feasible, at least in the dystrophic retina. Such enhanced cell delivery was also associated with potentially beneficial biochemical changes in the target tissue. The technique can be improved in a number of ways. Orbital space around the globe, especially in humans, allows for magnet placement in any chosen quadrant and also for much larger magnets to be used (e.g., to increase magnetic MSC delivery tangentially over the entire retinal surface). Flexible, Halbach array-type magnets might facilitate such orbital placement (15). Culturing MSCs in the presence of a magnetic field has also been suggested as a way of increasing their magnetic attractiveness and so enhance cell delivery (36,37). Most advantageously, systemic delivery of magnetized cells allows for repeat

treatments with less risk to the retina than that associated with injection of cells directly into the eye. Areas of tissue suboptimally treated could be targeted at subsequent visits simply by moving the underlying magnet. Genetic modification of MSCs would also allow for cells to deliver other therapeutic molecules to the diseased tissue (27).

In conclusion, our results show that large numbers of blood-borne magnetic MSCs can be targeted to specific retinal loci and produce therapeutically useful biochemical changes in the target tissue. Such an approach would therefore be optimal in focal tissue diseases of the outer retina such as age-related macular degeneration, where only a limited area of tissue is affected and direct injection of cells could lead to adverse collateral damage. With the range of therapeutic possibilities achievable with MSCs, their magnetic targeting potentially combines therapeutic versatility with the focused targeting needed to solve many of the cell delivery problems of future translational studies in diseased neurological tissues.

*ACKNOWLEDGMENTS:* This work was supported by grants from the Canadian Institutes of Health Research. The authors declare no conflicts of interest.

## REFERENCES

1. Arbab, A. S.; Jordan, E. K.; Wilson, L. B.; Yocum, G. T.; Lewis, B. K.; Frank, J. A. *In vivo* trafficking and targeted delivery of magnetically labeled stem cells. *Hum. Gene Ther.* 15:351–360; 2004.
2. Arnhold, S.; Klein, H.; Semkova, I.; Addicks, K.; Schraermeyer, U. Neurally selected embryonic stem cells induce tumor formation after long-term survival following engraftment into the subretinal space. *Invest. Ophthalmol. Vis. Sci.* 45:4251–4255; 2004.
3. Baker, P. S.; Brown, G. C. Stem-cell therapy in retinal disease. *Curr. Opin. Ophthalmol.* 20:175–181; 2009.
4. Balakumaran, A.; Pawelczyk, E.; Ren, J.; Sworder, B.; Chaudhry, M.; Sabatino, M.; Stroncek, D.; Frank, J. A.; Robey, P. G. Superparamagnetic iron oxide nanoparticles labeling of bone marrow stromal (mesenchymal) cells does not affect their “stemness”. *PLoS One* 5:e11462; 2010.
5. Berson, E. L.; Rosner, B.; Weigel-DiFranco, C.; Dryja, T. P.; Sandberg, M. A. Disease progression in patients with dominant retinitis pigmentosa and rhodopsin mutations. *Invest. Ophthalmol. Vis. Sci.* 43:3027–3036; 2002.
6. Castanheira, P.; Torquetti, L. T.; Magalhães, D. R.; Nehemy, M. B.; Goes, A. M. DAPI diffusion after intravitreal injection of mesenchymal stem cells in the injured retina of rats. *Cell Transplant.* 18:423–431; 2009.
7. Chen, H.; Kaminski, M. D.; Pytel, P.; Macdonald, L.; Rosengart, A. J. Capture of magnetic carriers within large arteries using external magnetic fields. *J. Drug Target.* 16: 262–268; 2008.
8. Chen, J.; Makino, C. L.; Peachey, N. S.; Baylor, D. A.; Simon, M. I. Mechanisms of rhodopsin inactivation *in vivo* as revealed by a COOH-terminal truncation mutant. *Science* 267:374–377; 1995.

9. Coletti, D.; Teodori, L.; Albertini, M. C. Static magnetic fields enhance skeletal muscle differentiation in vitro by improving myoblast alignment. *Cytometry A*. 71:846–856; 2007.
10. Congdon, N.; O'Colmain, B.; Klaver, C. C.; Klein, R.; Munoz, B.; Friedman, D. S.; Kempen, J.; Taylor, H. R.; Mitchell, P. Eye diseases prevalence research group. Causes and prevalence of visual impairment among adults in the United States. *Arch. Ophthalmol.* 122:477–485; 2004.
11. Gregory-Evans, K.; Chang, F.; Hodges, M. D.; Gregory-Evans, C. Y. Ex vivo gene therapy using intravitreal injection of GDNF-secreting mouse embryonic stem cells in a rat model of retinal degeneration. *Mol. Vis.* 15:962–973; 2009.
12. Grierson, I.; Rahi, A. H. Structural basis of contraction in vitreal fibrous membranes. *Br. J. Ophthalmol.* 65:737–749; 1981.
13. Guerin, K.; Gregory-Evans, C. Y.; Hodges, M. D.; Moosajee, M.; Mackay, D. S.; Gregory-Evans, K.; Flannery, J. G. Systemic aminoglycoside treatment in rodent models of retinitis pigmentosa. *Exp. Eye Res.* 87:197–207; 2008.
14. Hafeli, U. O.; Pauer, G. J. In vitro and in vivo toxicity of magnetic nanoparticles. *J. Magn. Magn. Mater.* 194: 76–82; 1999.
15. Halbach, K. Design of permanent multipole magnets with oriented rare earth cobalt material. *Nucl. Instrum. Methods* 169:1–10; 1980.
16. Hamasaki, T.; Tanaka, N.; Kamei, N. Magnetically labeled neural progenitor cells, which are localized by magnetic force, promote axon growth in organotypic cocultures. *Spine* 32:2300–2305; 2007.
17. Hayden, M. E.; Häfeli, U. O. Magnetic bandages for targeted delivery of therapeutic agents. *J. Phys. Cond. Matter* 18:S2877–2891; 2006.
18. Joe, A. W.; Gregory-Evans, K. Mesenchymal stem cells and potential applications in treating ocular disease. *Curr. Eye Res.* 35:941–952; 2010.
19. Johnson, T. V.; Bull, N. D.; Hunt, D. P.; Marina, N.; Tomarev, S. I.; Martin, K. R. Neuroprotective effects of intravitreal mesenchymal stem cell transplantation in experimental glaucoma. *Invest. Ophthalmol. Vis. Sci.* 51: 2051–2059; 2010.
20. Kulbatski, I. Stem/precursor cell-based CNS therapy: The importance of circumventing immune suppression by transplanting autologous cells. *Stem Cell. Rev.* 6:405–410; 2010.
21. Kyrtatos, P. G.; Lehtolainen, P.; Junemann-Ramirez, M.; Garcia-Prieto, A.; Price, A. N.; Martin, J. F.; Gadian, D. G.; Pankhurst, Q. A.; Lythgoe, M. F. Magnetic tagging increases delivery of circulating progenitors in vascular injury. *JACC Cardiovasc. Interv.* 2:794–802; 2009.
22. Loebinger, M. R.; Kyrtatos, P. G.; Turmaine, M.; Price, A. N.; Pankhurst, Q.; Lythgoe, M. F.; Janes, S. M. Magnetic resonance imaging of mesenchymal stem cells homing to pulmonary metastases using biocompatible magnetic nanoparticles. *Cancer Res.* 69:8862–8867; 2009.
23. Lu, B.; Wang, S.; Girman, S.; McGill, T.; Ragaglia, V.; Lund, R. Human adult bone marrow-derived somatic cells rescue vision in a rodent model of retinal degeneration. *Exp. Eye Res.* 91:449–455; 2010.
24. Marchetti, V.; Krohne, T. U.; Friedlander, D. F.; Friedlander, M. Stemming vision loss with stem cells. *J. Clin. Invest.* 120:3012–3021; 2010.
25. Marchi, N.; Teng, Q.; Nguyen, M. T.; Franic, L.; Desai, N. K.; Masaryk, T.; Rasmussen, P.; Trasciatti, S.; Janigro, D. Multimodal investigations of trans-endothelial cell trafficking under condition of disrupted blood–brain barrier integrity. *BMC Neurosci.* 11:34; 2010.
26. Monzen, S.; Takahashi, K.; Toki, T. Exposure to a MRI-type high-strength static magnetic field stimulates megakaryocytic/erythroid hematopoiesis in CD34(+) cells from human placental and umbilical cord blood. *Bioelectromagnetics* 30:280–285; 2009.
27. Myers, T. J.; Granero-Molto, F.; Longobardi, L.; Li, T.; Yan, Y.; Spagnoli, A. Mesenchymal stem cells at the intersection of cell and gene therapy. *Expert Opin. Biol. Ther.* 10:1663–1679; 2010.
28. Nagai, N.; Kawao, N.; Okada, K.; Okumoto, K.; Teramura, T.; Ueshima, S.; Umemura, K.; Matsuo, O. Systemic transplantation of embryonic stem cells accelerates brain lesion decrease and angiogenesis. *Neuroreport* 21:575–579; 2010.
29. Nishida, K.; Tanaka, N.; Nakanishi, K.; Kamei, N.; Hamasaki, T.; Yanada, S.; Mochizuki, Y.; Ochi, M. Magnetic targeting of bone marrow stromal cells into spinal cord: Through cerebrospinal fluid. *Neuroreport* 17:1269–1272; 2006.
30. Parekkadan, B.; Milwid, J. M. Mesenchymal stem cells as therapeutics. *Ann. Rev. Biomed. Eng.* 12:87–117; 2010.
31. Pearson, R. A.; Barber, A. C.; West, E. L.; MacLaren, R. E.; Duran, Y.; Bainbridge, J. W.; Sowden, J. C.; Ali, R. R. Targeted disruption of outer limiting membrane junctional proteins (Crb1 and ZO-1) increases integration of transplanted photoreceptor precursors into the adult wild-type and degenerating retina. *Cell Transplant.* 19: 487–503; 2010.
32. Pislaru, S. V.; Harbuzariu, A.; Gulati, R.; Witt, T.; Sandhu, N. P.; Simari, R. D.; Sandhu, G. S. Magnetically targeted endothelial cell localization in stented vessels. *J. Am. Coll. Cardiol.* 48:1839–1845; 2006.
33. Polyak, B.; Fishbein, I.; Chorny, M.; Alferiev, I.; Williams, D.; Yellen, B.; Friedman, G.; Levy, R. J. High field gradient targeting of magnetic nanoparticle-loaded endothelial cells to the surfaces of steel stents. *Proc. Natl. Acad. Sci. USA* 105:698–703; 2008.
34. Riegler, J.; Wells, J. A.; Kyrtatos, P. G.; Price, A. N.; Pankhurst, Q. A.; Lythgoe, M. F. Targeted magnetic delivery and tracking of cells using a magnetic resonance imaging system. *Biomaterials* 31:5366–5371; 2010.
35. Schäfer, R.; Ayturan, M.; Bantleon, R. The use of clinically approved small particles of iron oxide (SPIO) for labeling of mesenchymal stem cells aggravates clinical symptoms in experimental autoimmune encephalomyelitis and influences their in vivo distribution. *Cell Transplant.* 17:923–941; 2008.
36. Schäfer, R.; Bantleon, R.; Kehlbach, R.; Siegel, G.; Wiskirchen, J.; Wolburg, H.; Kluba, T.; Eibofner, F.; Northoff, H.; Claussen, C. D.; Schlemmer, H. P. Functional investigations on human mesenchymal stem cells exposed to magnetic fields and labeled with clinically approved iron nanoparticles. *BMC Cell Biol.* 11:22; 2010.
37. Schäfer, R.; Kehlbach, R.; Müller, M. Labeling of human mesenchymal stromal cells with superparamagnetic iron oxide leads to a decrease in migration capacity and colony formation ability. *Cytotherapy* 11:68–78; 2009.
38. Schäfer, R.; Kehlbach, R.; Wiskirchen, J. Transferin receptor upregulation: In vitro labeling of rat

- mesenchymal stem cells with superparamagnetic iron oxide. *Radiology* 244:514–523; 2007.
39. Solomon, S. D.; Dong, L. M.; Haller, J. A.; Gilson, M. M.; Bressler, N. M.; SST research group and the SST adverse event review committee. Risk factors for rhegmatogenous retinal detachment in the submacular surgery trials: SST report No. 22. *Retina* 29:819–824; 2009.
  40. Steinberg, R. H.; Flannery, J. G.; Naash, M.; LaVail, M. M. Transgenic rat models of inherited retinal degeneration caused by mutant opsin genes. *Invest. Ophthalmol. Vis. Sci.* 37(Suppl.):698; 1996.
  41. Tang, C.; Russell, P. J.; Martiniello-Wilks, R.; Rasko, J. E.; Khatri, A. Concise review: Nanoparticles and cellular carriers-allies in cancer imaging and cellular gene therapy? *Stem Cells* 28:1686–1702; 2010.
  42. Tiefenauer, L. X. Magnetic nanoparticles as contrast agents for medical diagnosis. In: Vo-Dinh, T., ed. *Nanotechnology in biology and medicine: Methods, devices, and applications*. Boca Raton, FL: CRC Press; 2007:1–20.
  43. Wang, H. C.; Brown, J.; Alayon, H.; Stuck, B. E. Transplantation of quantum dot-labelled bone marrow-derived stem cells into the vitreous of mice with laser-induced retinal injury: Survival, integration and differentiation. *Vision Res.* 50:665–673; 2010.
  44. Wang, S.; Lu, B.; Girman, S.; Duan, J.; McFarland, T.; Zhang, Q. S.; Grompe, M.; Adamus, G.; Appukuttan, B.; Lund, R. Non-invasive stem cell therapy in a rat model for retinal degeneration and vascular pathology. *PLoS One* 5:e9200; 2010.
  45. Wilhelm, C.; Bal, L.; Smirnov, P.; Galy-Fauroux, I.; Clément, O.; Gazeau, F.; Emmerich, J. Magnetic control of vascular network formation with magnetically labeled endothelial progenitor cells. *Biomaterials* 28:3797–3806; 2007.
  46. Yagi, H.; Soto-Gutierrez, A.; Parekkadan, B.; Kitagawa, Y.; Tompkins, R. G.; Kobayashi, N.; Yarmush, M. L. Mesenchymal stem cells: Mechanisms of immunomodulation and homing. *Cell Transplant.* 19:667–679; 2010.
  47. Zhang, Y.; Wang, W. Effects of bone marrow mesenchymal stem cell transplantation on light-damaged retina. *Invest. Ophthalmol. Vis. Sci.* 51:3742–3748; 2010.